A SARS-CoV2 Model For Informing E-II Policy

Kevin Shen, Sally Jiao

June 2020

1 Abstract

We have built a mechanistic model of infectious disease dynamics to better assess how observables (e.g. R_0, infectious case load) are connected to "microscopic" parameters that can be controlled. The model can help answer questions like: the efficacy of different quarantine protocols, and the relative risk of SARS-CoV2 spread in E-II relative to in the greater Santa Barbara community. With more microscopic data we can also try to infer more fundamental quantities, such as the risk per unit time of close contact.

2 The Model

We have coupled an agent-based model (individual-level resolution) of E-II scheduling and disease dynamics, based on the Imperial College London model [1, 2], with a simplified model of Santa Barbara disease dynamics based on the SIR model. The modeling of the greater Santa Barbara background infection rate is meant to include both intra-home and greater-community (e.g. grocery shopping) effects.

The agent-based model allows fine-grained control over:

1. Lab group assignment, size, etc. (currently performed randomly)
2. Biological factors: distributions over disease histories, individual infectiousness, asymptomatic vs. symptomatic people
3. Quarantine, scheduling (currently performed randomly), and mask-wearing protocols
4. Rate of "background" infections in E-II (infections not due to close contact with a group member in E-II) and parameters controlling dynamics of "community" spread.

There are several "microscopic" variables, such as the infection risk per unit time of close contact, the rate at which two individuals come into close contact, PPE factors, etc. For initial exploration, we parameterize the model such that "business as usual", with no lab scheduling nor PPE, results in $R_0 \approx 1.31 \pm 0.035$. Due to a distribution of group sizes and inherent stochasticity of infection, the standard deviation is 1.11. Justification for this calibration is given in the Appendix, though the R_0^{EII} baseline can be adjusted to examine other scenarios/prior beliefs of infection risk in E-II.

3 Preliminary Calculations and Observations

We first characterize the baseline distribution of secondary cases for full-capacity operations, with an intra-E-II R_0 of 1.3. The model was run 1000 times and quantities were averaged over all runs. There is significant

variation in the number of secondary infections in this "business as usual" scenario, even though the average number of secondary infections is relatively low.

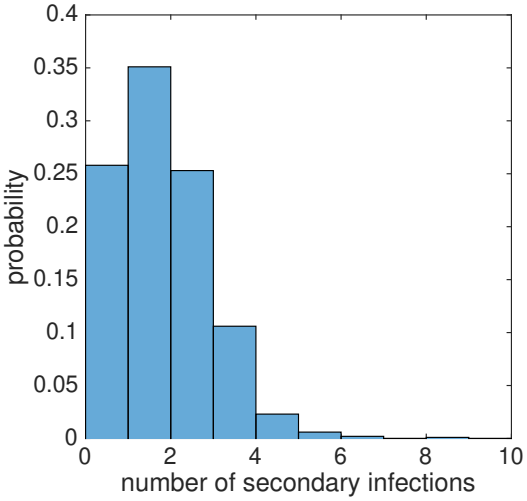

We also compute the total number of infections (secondary infections + infections from further spread) resulting from a single infected E-II worker. Stricter quarantining policies reduce the total number of infections. Here, we compare no quarantining, as in the "business as usual" scenario outlined above, to a simple quarantine policy where only people exhibiting symptoms are quarantined, to stricter policies where labs of newly symptomatic people are shut down for a number of days. The drop in number of infections with the implementation of any quarantine policy and subsequent smaller drop with the severity of the policy is consistent with results from other transmission models [5]. The model was run for 50 days and quantities were averaged over 100 runs. Here, we do not account for fomite build-up; the only direct intra-lab transmission is through person-to-person contact. We can incorporate a model of fomite build-up and its effect on transmission into a future version of the E-II model. Accounting for this would increase the number of intra-lab infections in the "business-as-usual" scenario and therefore likely increase the effectiveness of lab shutdowns.

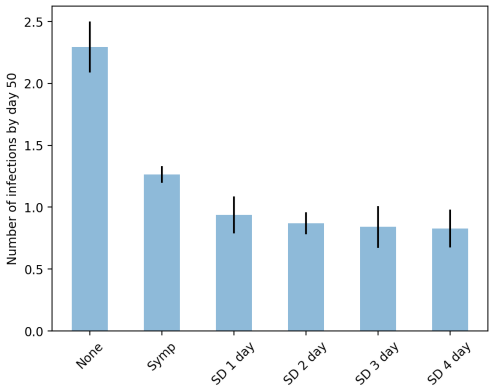

(a) Average number of cases by day 50

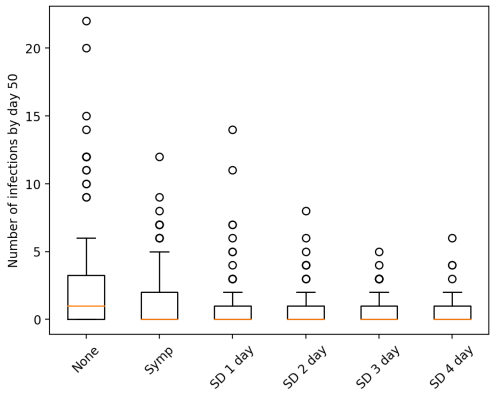

(b) Variation in number of cases by day 50 over 100 model runs

We can also explore the effect of Santa Barbara in driving the disease. Assume that, in the community, individuals are out and actively infecting for 4 days, with a background community R_0 of 1.08 (California's current virus reproduction rate [6]). We seed the community with the current Santa Barbara fraction of

active cases ≈ 0.005, and study a fairly lax scenario: E-II at 50% capacity with a simple quarantine policy where only symptomatic people are quarantined, but their labs are not.

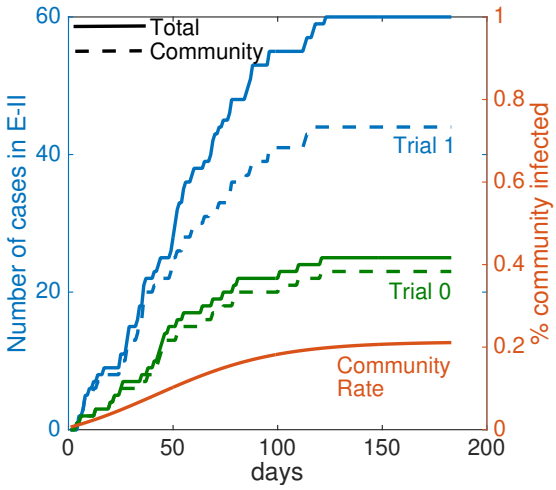

In the last figure we present two different random simulations with the same initial conditions. Solid (blue and green) lines are the total number of cases in the E-II population, and dashed lines are the cases that arise from community infection instead of from intra-E-II spread. The red line shows the fraction of the greater Santa Barbara community that has been infected. In this scenario, the community value of $R_0^{\text{community}} = 1.08$ leads to slow infection dynamics, and a relatively low plateau (roughly 20% infected), provided this low rate of infection can be sustained over 6 months.

Importantly, many of the infections are driven by the community. Another important observation is that there is significant stochasticity and variation in the total number of people infected, and also in the fraction of infections in the E-II population that arise from the greater community versus intra-E-II. This variance will be important to understand for appropriate risk analysis and management.

4 Observations and Future Work

Initial calculations and parameterizations highlight two features. First, there is significant stochasticity in the number of secondary cases, implying that variances, and not just average behavior, should be accounted for in planning. Secondly, the simple quarantine protocols considered thus far have modest impacts on the disease trajectory. At the conditions considered, much of the infection case load is driven by community infections. Furthermore, it is consistent with observations that presymptomatic spread can play a large role, and that timely contact tracing and pre-emptive quarantining policies are critical [3]. Further study of parameter space and quarantine protocols is required to understand the generality of these observations.

Future work with the model will include more realistic handling of lab group assignment and scheduling (currently performed randomly). We can also incorporate or validate against E-II measurables (e.g. any existing information about spread) to improve the model's ability to compare various containment policies.

5 Appendix

5.1 Models of disease dynamics

The essential assumption of the Ferguson et al. model is an exponential dose-response relationship:

$$P_{\text{infect}}(\Delta T) = 1 - \exp(-\lambda d(\Delta T)) \tag{1}$$

where $P_{\text{infect}}(\Delta T)$ is the probability that someone is infected in an interval of length ΔT after exposure to a dose $d(\Delta T)$, and λ is an empirical factor.

The essential assumption of the SIR model used to treat Santa Barbara dynamics is the assumption of random mixing, which is suitable for modeling a population on average. In the SIR model, the infection rate of each susceptible person is simply:

$$r_{\text{infect}} = \beta i(t) \tag{2}$$

where $i(t)$ is the fraction of the Santa Barbara community that is actively infectious, and β is a rate constant modeling the transmission rate. This is coupled to the agent-based model as a background infection rate when the individual is not working in E-II.

The model can be augmented to account for build-up of environmental risk, e.g. fomites, but that has not yet been considered in these preliminary studies.

5.2 Virus Biology

Our model of disease progression is taken from He et al. [4], who tracked viral shedding and symtom profiles as a function of time. Viral shedding is approximated with linear ramp functions, reaching peak infectivity 2 days after infection, followed by a gradual decline to zero infectivity 9 days after infection (the real shedding profile has a low but longer tail out to days 12∼14). Meanwhile, we model symptoms with a step function, appearing on day 3, and persisting until day 14. The asymptomatic rate is taken to be 25%, and results in an infectivity reduction factor of 0.5. Finally, post-infection immunity is assumed over the duration of the conducted simulations (the longest of which is 6 months).

5.3 Calibration, parameterization

Our model calibration to R_0^{EII} is performed as follows:

1. assuming: an average group size of 10, and that virus risk in public spaces (i.e. hallways, stairways) is a factor of 100 lower than intra-lab infectious contacts.
2. $R_0^{EII} \approx 1.3$ is roughly consistent with modeling $R_0 = R_0^{\text{non-work-related}} + R_0^{\text{work}}$. Assuming the current California shutdown policies have essentially set $R_0^{\text{work,NPI}} = 0$, we estimate average $R_0^{\text{community}} \approx R_0^{\text{NPI}} \approx 1.1$ (roughly California's current R_0). Then, noting that R_0^{noNPI} has conservatively been estimated to be 2.5, we estimate that the "business-as-usual" R_0^{work} is around 1.4.

5.4 Distribution of R_0

To further emphasize the broad distribution of possible secondary infections, we present box plots at different occupation levels of E-II. The mean is indicated by the dashed line running across different occupation fractions. Outliers are visualized using jitter to represent their frequency. These outliers are probably associated with larger groups. The data here is a "worst case" scenario: no quarantines are implemented. In the future, we can modulate infectiousness by lab size, or implement refined scheduling policies.

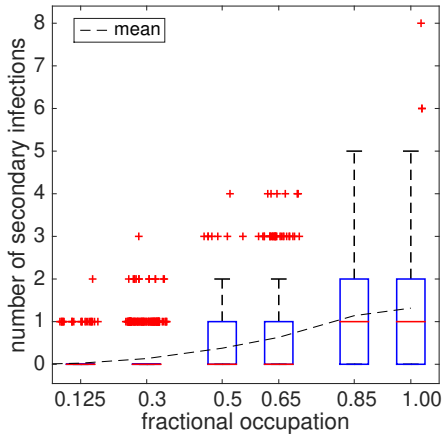

5.5 Importance of mask-wearing

To quantify the effects of mask-wearing, we scale the infected individual's infectiousness by a factor from 0 to 1. In the "business-as-usual" scenario, R_0 is approximately linear with this scale factor, suggesting, unsurprisingly, that any reductions in infectiousness due to mask-wearing directly translate to a reduction in the disease spread. For instance, a 50% reduction in infectiousness in the absence of any quarantining has the same effect on R_0 as quarantining symptomatics (a 45% reduction in R_0 from 1.3 to 0.72). If we were to also account for the protective effects of mask-wearing on non-infected individuals, we would expect the number of secondary infections to be further reduced.

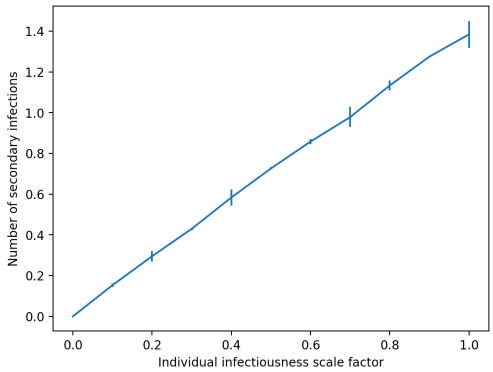

5.6 Computational Expense

The computational expense of running the model scales slightly supralinearly with respect to the total number of E-II occupants ($O(N^{1.2})$), slightly sublinearly with respect to the fraction of people working ($O(N^{0.9})$) and linearly with respect to the number of steps (e.g. days) run.

References

[1] N. M. Ferguson, D. A. T. Cummings, S. Cauchemez, C. Fraser, S. Riley, A. Meeyai, S. Iamsirithaworn, and D. S. Burke. Strategies for containing an emerging influenza pandemic in southeast asia. 437(7056):209–214.

[2] Ferguson, Neil, D. Laydon, G. Nedjati Gilani, N. Immai, K. Ainslie, M. Baguelin, S. Bhatia, A. Boonyasiri, Z. Cucunuba Perez, G. Cuomo-Dannenburg, and more... Report 9: Impact of non-pharmaceutical interventions (NPIs) to reduce COVID-19 mortality and healthcare demand. Mar. 2020.

[3] L. Ferretti, C. Wymant, M. Kendall, L. Zhao, A. Nurtay, L. Abeler-Dörner, M. Parker, D. Bonsall, and C. Fraser. Quantifying SARS-CoV-2 transmission suggests epidemic control with digital contact tracing. *Science*, 368(6491), May 2020.

[4] X. He, E. H. Y. Lau, P. Wu, X. Deng, J. Wang, X. Hao, Y. C. Lau, J. Y. Wong, Y. Guan, X. Tan, X. Mo, Y. Chen, B. Liao, W. Chen, F. Hu, Q. Zhang, M. Zhong, Y. Wu, L. Zhao, F. Zhang, B. J. Cowling, F. Li, and G. M. Leung. Temporal dynamics in viral shedding and transmissibility of COVID-19. 26(5):672–675.

[5] A. J. Kucharski, P. Klepac, A. J. K. Conlan, S. M. Kissler, M. L. Tang, H. Fry, J. R. Gog, W. J. Edmunds, J. C. Emery, G. Medley, J. D. Munday, T. W. Russell, Q. J. Leclerc, C. Diamond, S. R. Procter, A. Gimma, F. Y. Sun, H. P. Gibbs, A. Rosello, K. van Zandvoort, S. Hué, S. R. Meakin, A. K. Deol, G. Knight, T. Jombart, A. M. Foss, N. I. Bosse, K. E. Atkins, B. J. Quilty, R. Lowe, K. Prem, S. Flasche, C. A. B. Pearson, R. M. G. J. Houben, E. S. Nightingale, A. Endo, D. C. Tully, Y. Liu, J. Villabona-Arenas, K. O'Reilly, S. Funk, R. M. Eggo, M. Jit, E. M. Rees, J. Hellewell, S. Clifford, C. I. Jarvis, S. Abbott, M. Auzenbergs, N. G. Davies, and D. Simons. Effectiveness of isolation, testing, contact tracing, and physical distancing on reducing transmission of SARS-CoV-2 in different settings: a mathematical modelling study. page S1473309920304576.

[6] K. Systrom and T. Vladeck. R_t covid-19. `https://rt.live`, 2020. Accessed July 14, 2020.